

# Analysis of the Effects of Faraday Rotation on Spaceborne Polarimetric SAR Observations at P-Band

Ren-Yuan Qi and Ya-Qiu Jin, *Fellow, IEEE*

**Abstract**—Spaceborne microwave observation of subcanopy and subsurface requires the polarimetric synthetic aperture radar (SAR) technology at lower microwave frequencies, such as P-band. However, SAR observation at P-band is remarkably influenced by the Faraday rotation (FR) effect through the ionosphere. An example in this paper illustrates why the measured polarimetric data with FR at P-band cannot be directly applied to terrain surface classification. We further present that the parameters  $u$ ,  $\nu$ ,  $H$ ,  $\alpha$ ,  $A$  for terrain surface classification derived from the polarimetric data without FR, which are recovered from the data with FR, can be applied to the surface classification, there is a  $\pm\pi/2$  ambiguity error unresolved. Based on gradual change of the FR degree along a geographical location, a method to eliminate the  $\pm\pi/2$  ambiguity error is designed. Thus, the polarimetric scattering vector and Mueller matrix without FR and  $\pm\pi/2$  ambiguity can be fully inverted from the measured polarimetric data with FR.

**Index Terms**—Faraday rotation (FR), P-band polarimetric synthetic aperture radar (SAR), terrain surface classification.

## I. INTRODUCTION

**M**OISTURE profiles in subcanopy and subsurface (0 ~ 5 m) are key parameters for the studies of global change, land hydrological process, the global carbon balance, etc. To obtain these profiles is the main purpose of the microwave observation of subcanopy and subsurface [1]–[6]. In general case, synthetic aperture radar (SAR) technology employs the L-, C-, X-, or Ku-bands, which can monitor no-dense vegetation canopy (with  $\sim 4 \text{ kg/m}^2$  of biomass) and penetrate through the land media in the depth order about 10 cm or so, even at lowest L-band. It needs UHF/very high frequency (VHF) bands (435 MHz, 135 MHz) to penetrate through the dense subcanopy ( $\sim 20 \text{ kg/m}^2$  and more) with little scattering and reach subsurface. However, it has been known that the satellite-borne SAR measurements at UHF/VHF bands are significantly affected by the Faraday rotation (FR).

Polarization vectors of electromagnetic wave are rotated when the wave passes through the anisotropic ionosphere and action of geomagnetic field. This rotation is called the FR effect. The FR depends on the wavelength, electronic density, geomagnetic field, the angle between the direction of wave

propagation and geomagnetic field, and the wave incidence angle [7]. The FR may decrease the difference between copolarized ( $\nu\nu$  and  $hh$ ) backscattering, enhance cross-polarized echoes, and mix different polarized terms. Thus, the satellite-borne SAR data at low frequency becomes distorted due to FR effect.

Since the FR is proportional to the square power of the wavelength, it yields especially serious impact on the SAR observation operating at the frequency lower than L-band. The FR angle at P-band can reach dozens of degrees. Even for mono-polarized measurement with a known FR degree, the true scattering vector cannot be inverted from the observed SAR data [8].

Since pioneer experiment of spaceborne imaging radar—version C SAR in 1994, the satellite-borne advanced land observing satellite phase array polarimetric SAR at L-band has been launched in January 2006. Canadian Radarsat-2 polarimetric SAR at C-band will be in orbit in 2007. Polarimetric SAR will provide much richer information. As for the FR issue, Freeman [9] derived polarimetric  $2 \times 2$ -D (dimensional) complex scattering matrix without FR from SAR data with FR. But, he pointed out that there existed the  $\pm\pi/2$  ambiguity error to fully determine the scattering matrix without FR. This ambiguity error is remained to be resolved.

In this paper, an example shows how the P-band data with FR is distorted and why it cannot be directly applied to terrain surface classification. Then,  $4 \times 4$ -D Mueller matrix without FR is inverted from one with FR, and it shows that the remained  $\pm\pi/2$  ambiguity error does not affect the classification parameters:  $u$ ,  $\nu$ ,  $H$ ,  $\alpha$ ,  $A$  [10], [11]. This Mueller matrix without FR can be directly applied to surface classification, regardless to the  $\pm\pi/2$  ambiguity error. Based on intuitive assumption of gradual change of FR degree with geographical position, a method, as alternative approach from [9], to eliminate the  $\pm\pi/2$  ambiguity error is designed. Our example shows the polarimetric SAR without FR at low frequency, such as P-band, can be fully inverted.

## II. FR EFFECT FOR TERRAIN SURFACE CLASSIFICATION

As a polarized electromagnetic wave passes through the ionosphere, the polarization vectors are rotated because of FR effect. The FR angle is calculated as [7]

$$\Omega = \left( \frac{\pi}{cf^2} \right) \int f_p^2(s) f_B(s) \cos(\Theta_B(s)) ds \quad (1)$$

Manuscript received October 23, 2006; revised January 9, 2007. This work was supported by the National Science Foundation of China under Grants 40637033 and 60571050.

The authors are with the Key Laboratory of Wave Scattering and Remote Sensing Information (MOE), Fudan University, Shanghai 200433, China (e-mail: yqjin@fudan.ac.cn).

Digital Object Identifier 10.1109/TGRS.2007.892583

where  $f$  is the electromagnetic wave frequency,  $f_B$  is electronic gyrofrequency,  $f_p$  is the plasma frequency, and  $\Theta_B$  is the angle between the directions of electromagnetic wave propagation and geomagnetic field. It can be seen that as  $\Theta_B = 90^\circ$ , (1) yields  $FR = 0$  [12].

Assuming that the propagation direction is not changed passing through homogeneous ionosphere,  $ds = \sec \theta_i dz$  (where  $\hat{z}$  is the normal to the surface and  $\theta_i$  is the incident angle), and geomagnetic field keeps constant as one at 400-km altitude [7], (1) yields

$$\Omega_F \approx -2620 \rho_e B(400) \lambda^2 \cos \Theta_B \sec \theta_i [\text{radians}] \quad (2)$$

where  $\rho_e$  is the total electron content per unit area ( $10^{16}$  electron/m<sup>2</sup>), and  $B(400)$  is the intensity of geomagnetic field ( $T$ ) at 400-km altitude.

The scattering matrix with FR (indicated by superscript F) is written by the scattering matrix without FR as follows [13]:

$$\begin{aligned} S_{hh}^F &= S_{hh} \cos^2 \Omega - S_{\nu\nu} \sin^2 \Omega \\ S_{h\nu}^F &= S_{h\nu} + (S_{hh} + S_{\nu\nu}) \sin \Omega \cos \Omega \\ S_{\nu h}^F &= S_{h\nu} - (S_{hh} + S_{\nu\nu}) \sin \Omega \cos \Omega \\ S_{\nu\nu}^F &= -S_{hh} \sin^2 \Omega + S_{\nu\nu} \cos^2 \Omega \end{aligned} \quad (3)$$

where backscattering reciprocity is adopted.

Based on the assumption of reflection symmetry ( $\langle S_{hh} S_{h\nu}^* \rangle = \langle S_{h\nu} S_{\nu\nu}^* \rangle = 0$ ), Freeman derived a relationship between the Mueller matrices with FR and without FR [8]. However, as the scatters are not uniformly oriented in azimuthal direction, the assumption of so-called reflection symmetry is not true. Actually, keeping these two items, we derived the following Mueller matrix with FR, which have been independently addressed in an earlier paper [15]:

$$\begin{aligned} \langle S_{hh} S_{hh}^* \rangle^F &= \langle S_{hh} S_{hh}^* \rangle \cos^4 \Omega + \langle S_{\nu\nu} S_{\nu\nu}^* \rangle \sin^4 \Omega \\ &\quad - 2\text{Re} \langle S_{hh} S_{\nu\nu}^* \rangle \sin^2 \Omega \cos^2 \Omega \end{aligned} \quad (4a)$$

$$\begin{aligned} \langle S_{\nu\nu} S_{\nu\nu}^* \rangle^F &= \langle S_{\nu\nu} S_{\nu\nu}^* \rangle \cos^4 \Omega + \langle S_{hh} S_{hh}^* \rangle \sin^4 \Omega \\ &\quad - 2\text{Re} \langle S_{hh} S_{\nu\nu}^* \rangle \sin^2 \Omega \cos^2 \Omega \end{aligned} \quad (4b)$$

$$\begin{aligned} \langle S_{h\nu} S_{h\nu}^* \rangle^F &= \langle S_{h\nu} S_{h\nu}^* \rangle + (\text{Re} \langle S_{hh} S_{h\nu}^* \rangle + \text{Re} \langle S_{h\nu} S_{\nu\nu}^* \rangle) \\ &\quad \times \sin 2\Omega + (2\text{Re} \langle S_{hh} S_{\nu\nu}^* \rangle + \langle S_{hh} S_{hh}^* \rangle \\ &\quad + \langle S_{\nu\nu} S_{\nu\nu}^* \rangle) \sin^2 \Omega \cos^2 \Omega \end{aligned} \quad (4c)$$

$$\begin{aligned} \langle S_{\nu h} S_{\nu h}^* \rangle^F &= \langle S_{h\nu} S_{h\nu}^* \rangle - (\text{Re} \langle S_{hh} S_{h\nu}^* \rangle + \text{Re} \langle S_{h\nu} S_{\nu\nu}^* \rangle) \\ &\quad \times \sin 2\Omega + (2\text{Re} \langle S_{hh} S_{\nu\nu}^* \rangle + \langle S_{hh} S_{hh}^* \rangle \\ &\quad + \langle S_{\nu\nu} S_{\nu\nu}^* \rangle) \sin^2 \Omega \cos^2 \Omega \end{aligned} \quad (4d)$$

$$\begin{aligned} \text{Re} \langle S_{hh} S_{h\nu}^* \rangle^F &= \text{Re} \langle S_{hh} S_{h\nu}^* \rangle \cos^2 \Omega + \langle S_{hh} S_{hh}^* \rangle \sin \Omega \\ &\quad \times \cos^3 \Omega + \frac{1}{4} \text{Re} \langle S_{hh} S_{\nu\nu}^* \rangle \sin 4\Omega \\ &\quad - \langle S_{\nu\nu} S_{\nu\nu}^* \rangle \sin^3 \Omega \cos \Omega \\ &\quad - \text{Re} \langle S_{h\nu} S_{\nu\nu}^* \rangle \sin^2 \Omega \end{aligned} \quad (4e)$$

$$\begin{aligned} \text{Im} \langle S_{hh} S_{h\nu}^* \rangle^F &= \text{Im} \langle S_{hh} S_{h\nu}^* \rangle \cos^2 \Omega + \frac{1}{2} \text{Im} \langle S_{hh} S_{\nu\nu}^* \rangle \\ &\quad \times \sin 2\Omega + \text{Im} \langle S_{h\nu} S_{\nu\nu}^* \rangle \sin^2 \Omega \end{aligned} \quad (4f)$$

$$\begin{aligned} \text{Re} \langle S_{hh} S_{\nu\nu}^* \rangle^F &= -\langle S_{hh} S_{hh}^* \rangle \sin^2 \Omega \cos^2 \Omega + \text{Re} \langle S_{hh} S_{\nu\nu}^* \rangle \\ &\quad \times \cos^4 \Omega + \text{Re} \langle S_{hh} S_{\nu\nu}^* \rangle \sin^4 \Omega \\ &\quad - \langle S_{\nu\nu} S_{\nu\nu}^* \rangle \sin^2 \Omega \cos^2 \Omega \end{aligned} \quad (4g)$$

$$\text{Im} \langle S_{hh} S_{\nu\nu}^* \rangle^F = \text{Im} \langle S_{hh} S_{\nu\nu}^* \rangle \cos 2\Omega \quad (4h)$$

$$\begin{aligned} \text{Re} \langle S_{h\nu} S_{\nu\nu}^* \rangle^F &= \text{Re} \langle S_{h\nu} S_{\nu\nu}^* \rangle \cos^2 \Omega - \text{Re} \langle S_{hh} S_{h\nu}^* \rangle \sin^2 \Omega \\ &\quad - \langle S_{hh} S_{hh}^* \rangle \sin^3 \Omega \cos \Omega + \frac{1}{4} \text{Re} \langle S_{hh} S_{\nu\nu}^* \rangle \\ &\quad \times \sin 4\Omega + \langle S_{\nu\nu} S_{\nu\nu}^* \rangle \sin \Omega \cos^3 \Omega \end{aligned} \quad (4i)$$

$$\begin{aligned} \text{Im} \langle S_{h\nu} S_{\nu\nu}^* \rangle^F &= \text{Im} \langle S_{h\nu} S_{\nu\nu}^* \rangle \cos^2 \Omega + \text{Im} \langle S_{hh} S_{h\nu}^* \rangle \sin^2 \Omega \\ &\quad + \text{Im} \langle S_{hh} S_{\nu\nu}^* \rangle \sin \Omega \cos \Omega \end{aligned} \quad (4j)$$

$$\begin{aligned} \text{Re} \langle S_{hh} S_{\nu h}^* \rangle^F &= \text{Re} \langle S_{hh} S_{h\nu}^* \rangle \cos^2 \Omega - \langle S_{hh} S_{hh}^* \rangle \\ &\quad \times \sin \Omega \cos^3 \Omega - \frac{1}{4} \text{Re} \langle S_{hh} S_{\nu\nu}^* \rangle \\ &\quad \times \sin 4\Omega + \langle S_{\nu\nu} S_{\nu\nu}^* \rangle \sin^3 \Omega \cos \Omega \\ &\quad - \text{Re} \langle S_{h\nu} S_{\nu\nu}^* \rangle \sin^2 \Omega \end{aligned} \quad (4k)$$

$$\begin{aligned} \text{Im} \langle S_{hh} S_{\nu h}^* \rangle^F &= \text{Im} \langle S_{hh} S_{h\nu}^* \rangle \cos^2 \Omega - \frac{1}{2} \text{Im} \langle S_{hh} S_{\nu\nu}^* \rangle \\ &\quad \times \sin 2\Omega + \text{Im} \langle S_{h\nu} S_{\nu\nu}^* \rangle \sin^2 \Omega \end{aligned} \quad (4l)$$

$$\begin{aligned} \text{Re} \langle S_{\nu h} S_{\nu\nu}^* \rangle^F &= \text{Re} \langle S_{h\nu} S_{\nu\nu}^* \rangle \cos^2 \Omega - \text{Re} \langle S_{hh} S_{h\nu}^* \rangle \\ &\quad \times \sin^2 \Omega + \langle S_{hh} S_{hh}^* \rangle \sin^3 \Omega \cos \Omega \\ &\quad - \frac{1}{4} \text{Re} \langle S_{hh} S_{\nu\nu}^* \rangle \sin 4\Omega \\ &\quad - \langle S_{\nu\nu} S_{\nu\nu}^* \rangle \sin \Omega \cos^3 \Omega \end{aligned} \quad (4m)$$

$$\begin{aligned} \text{Im} \langle S_{\nu h} S_{\nu\nu}^* \rangle^F &= \text{Im} \langle S_{h\nu} S_{\nu\nu}^* \rangle \cos^2 \Omega + \text{Im} \langle S_{hh} S_{h\nu}^* \rangle \sin^2 \Omega \\ &\quad - \text{Im} \langle S_{hh} S_{\nu\nu}^* \rangle \sin \Omega \cos \Omega \end{aligned} \quad (4n)$$

$$\begin{aligned} \text{Re} \langle S_{h\nu} S_{\nu h}^* \rangle^F &= \langle S_{h\nu} S_{h\nu}^* \rangle - (\langle S_{hh} S_{hh}^* \rangle + \langle S_{\nu\nu} S_{\nu\nu}^* \rangle) \\ &\quad + 2\text{Re} \langle S_{hh} S_{\nu\nu}^* \rangle \sin^2 \Omega \cos^2 \Omega \end{aligned} \quad (4o)$$

$$\text{Im} \langle S_{h\nu} S_{\nu h}^* \rangle^F = (\text{Im} \langle S_{hh} S_{h\nu}^* \rangle - \text{Im} \langle S_{h\nu} S_{\nu\nu}^* \rangle) \sin 2\Omega \quad (4p)$$

where  $\langle g \rangle$  denotes the ensemble average. It can be seen that each term of the Mueller matrix with FR is composed by different polarized elements of the Mueller matrix without FR. Also, the FR periodicity is  $180^\circ$ .

Fig. 1 gives a photo of Tabernash, CO (center location:  $39^\circ 98' \text{ N}$ ,  $105^\circ 50' \text{ W}$ ). Fig. 2 is the Jet Propulsion Laboratories airborne synthetic aperture radar (AIRSAR) image at P-band in that location (February 21, 2002). It is an airborne SAR image without any FR. Now, we suppose to move this SAR antenna to the satellite and impose FR effect on polarimetric AIRSAR data following (4a)–(4p).

In this example, the satellite is supposed be at 675-km altitude with looking to the east, total electron content follows the list of International Reference Ionosphere (IRI 2001),<sup>1</sup> and geomagnetic field is based on International Geomagnetic

<sup>1</sup> See <http://modelweb.gsfc.nasa.gov/models/iri.html>.



Fig. 1. Photo of the area Tabernash, CO (from Google Earth).

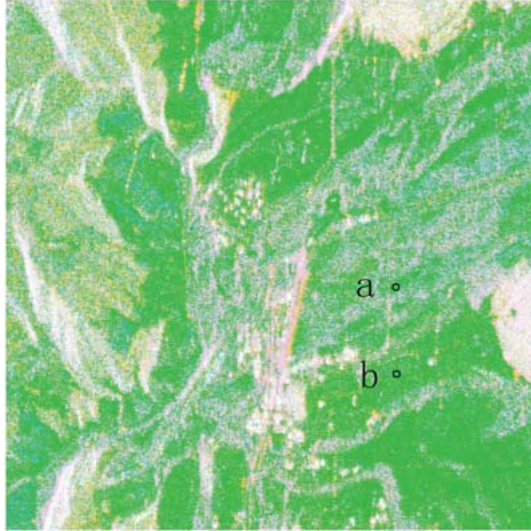


Fig. 2. AIRSAR image at P-band (Red = HH, Green = HV, Blue = VV).

Reference Field.<sup>2</sup> Fig. 3 shows temporal change of total electron content. Geomagnetic induction intensity is 44 413.1 nT with magnetic declination degree 10.2° and magnetic inclination degree 66.9°.

It is derived in (2) that  $\Theta_B$  is calculated as

$$\cos \Theta_B = \cos \theta_i \sin \Theta + \sin \theta_i \cos \Theta \sin \Phi \quad (5)$$

where  $\Theta$  is the magnetic inclination angle, and  $\Phi$  is the magnetic declination angle.

Following  $\rho_e$  of Fig. 3, i.e.,  $6 \sim 47.5 \times 10^{16}$  electron/m<sup>2</sup>, FR degree is  $16.4 \sim 129.6^\circ$  ( $\lambda = 0.857$  m). All terms of (4a)–(4p),  $\langle S_{pq} S_{rt}^* \rangle^F$ , are calculated with FR = 30°. Fig. 2, now with FR, becomes Fig. 4.

An example of an application that is strongly affected by FR is land cover classification. As a conventional approach, the parameters of  $\alpha$ ,  $A$  and the entropy  $H$  [10] have been applied

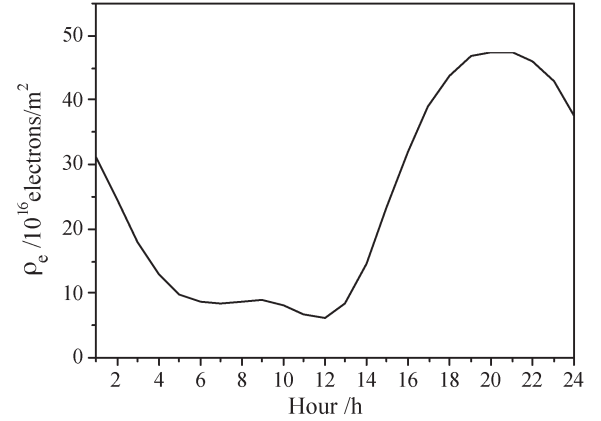
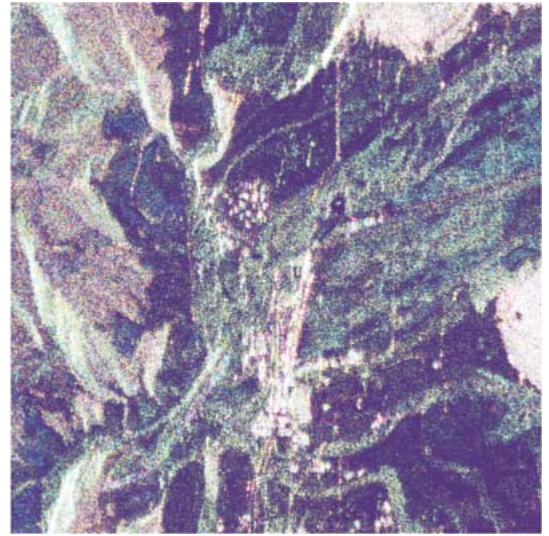

 Fig. 3. Temporal change of total electron content ( $\rho_e$ ) per unit area.


Fig. 4. Same AIRSAR image from Fig. 2, now distorted by an FR angle of 30° (color coding is the same).

to surface classification. Recently, the deorientation concept was introduced to reduce the influence of randomly fluctuating orientation and shows the prominence of targets' generic characteristics for terrain surface classification [11]. Making the target orientation into such a fixed state with minimization of cross-polarization, a set of the parameters  $u$ ,  $\nu$ ,  $\Psi$  are defined from deorientation of the principal scattering vector of random scatter targets. All these parameters as well as the entropy  $H$  are applied to terrain surface classification [11].

Using the parameters  $u$ ,  $\nu$ ,  $H$  for terrain surface classification, Fig. 5(a) is obtained from Fig. 2 without FR. As a comparison, Fig. 5(b) is classification from Fig. 4 with FR. These two classifications are totally different. For instance, the flat soil land of points a and b in Fig. 2 with weak scattering in Fig. 5(a) is misclassified as urban area with strong scattering in Fig. 5(b).

Fig. 6 shows change of the classification parameters  $u$ ,  $\nu$ ,  $H$  with FR degree at the point b of Fig. 2. It can be seen that the set of parameters ( $u < 0.3$ ,  $\nu > 0.2$ ,  $H < 0.5$ ) without FR is for the class of surface 3 (flat soil land), but FR30° makes the parameters as ( $u > 0.7$ ,  $\nu < -0.2$ ,  $H < 0.5$ ) and leads misclassification as urban 1. The parameters of  $u$ ,  $\nu$  are very sensitive to FR degree. Consequence is that the P-band

<sup>2</sup>See <http://modelweb.gsfc.nasa.gov/models/igrf.html>.



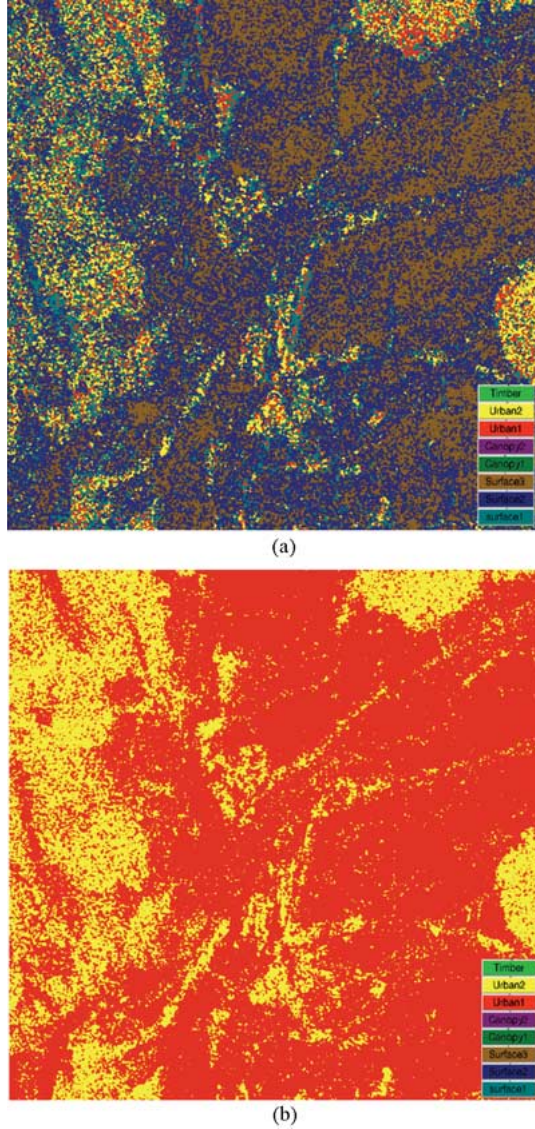


Fig. 5. (a) Terrain surface classification from Fig. 2. (b) Terrain surface classification from Fig. 4.

polarimetric data with FR cannot be directly applied to terrain surface classification.

### III. RECOVERING MUELLER MATRIX AND THE AMBIGUITY ERROR $\pm\pi/2$

From (3), Freeman [9] obtained

$$\Omega = \frac{1}{2} \tan^{-1} \left[ \frac{S_{h\nu}^F - S_{\nu h}^F}{S_{hh}^F + S_{\nu\nu}^F} \right]. \quad (6)$$

The scattering matrix without FR,  $[\tilde{S}_{pq}]$  ( $p, q = h, \nu$ ), is obtained from  $[S_{pq}^F]$  with FR as follows:

$$\begin{bmatrix} \tilde{S}_{hh} & \tilde{S}_{h\nu} \\ \tilde{S}_{\nu h} & \tilde{S}_{\nu\nu} \end{bmatrix} = \begin{bmatrix} \cos \Omega & -\sin \Omega \\ \sin \Omega & \cos \Omega \end{bmatrix} \times \begin{bmatrix} S_{hh}^F & S_{h\nu}^F \\ S_{\nu h}^F & S_{\nu\nu}^F \end{bmatrix} \begin{bmatrix} \cos \Omega & -\sin \Omega \\ \sin \Omega & \cos \Omega \end{bmatrix}. \quad (7)$$

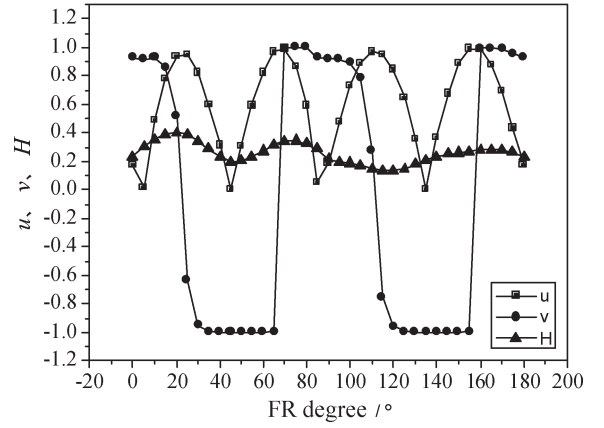


Fig. 6. Change of classification parameters ( $u, v, H$ ) with the FR degree.

It yields

$$\tilde{S}_{hh} = S_{hh}^F \cos^2 \Omega - S_{\nu\nu}^F \sin^2 \Omega + \frac{1}{2} (S_{h\nu}^F - S_{\nu h}^F) \sin 2\Omega \quad (8a)$$

$$\tilde{S}_{h\nu} = S_{h\nu}^F \cos^2 \Omega + S_{\nu h}^F \sin^2 \Omega - \frac{1}{2} (S_{hh}^F + S_{\nu\nu}^F) \sin 2\Omega \quad (8b)$$

$$\tilde{S}_{\nu h} = S_{\nu h}^F \cos^2 \Omega + S_{h\nu}^F \sin^2 \Omega + \frac{1}{2} (S_{hh}^F + S_{\nu\nu}^F) \sin 2\Omega \quad (8c)$$

$$\tilde{S}_{\nu\nu} = S_{\nu\nu}^F \cos^2 \Omega - S_{hh}^F \sin^2 \Omega + \frac{1}{2} (S_{h\nu}^F - S_{\nu h}^F) \sin 2\Omega. \quad (8d)$$

According to (3), an alternative method to recover cross-polarized items is given as

$$S_{h\nu} = S_{\nu h} = \frac{S_{h\nu}^F + S_{\nu h}^F}{2}. \quad (9)$$

If only measured Mueller matrix data are available, the FR degree can be equally derived from (4a)–(4p) as

$$\Omega = \frac{1}{2} \tan^{-1} \left[ \frac{\text{Im} \langle S_{hh} S_{h\nu}^* \rangle^F - \text{Im} \langle S_{hh} S_{\nu h}^* \rangle^F}{\text{Im} \langle S_{hh} S_{\nu\nu}^* \rangle^F} \right]. \quad (10)$$

Two other techniques, based on combinations of Mueller matrix terms, were also presented in [9, eqs. (12)–(15)].

The polarimetric Mueller matrix without FR can be inverted as

$$\begin{aligned} \langle S_{hh} S_{hh}^* \rangle &= \langle S_{hh} S_{hh}^* \rangle^F \cos^4 \Omega + \langle S_{\nu\nu} S_{\nu\nu}^* \rangle^F \sin^4 \Omega \\ &\quad - 2 \text{Re} \langle S_{hh} S_{\nu\nu}^* \rangle^F \sin^2 \Omega \cos^2 \Omega \\ &\quad + 2 \left( \text{Re} \langle S_{hh} S_{h\nu}^* \rangle^F - \text{Re} \langle S_{hh} S_{\nu h}^* \rangle^F \right) \\ &\quad \times \sin \Omega \cos^3 \Omega \\ &\quad - 2 \left( \text{Re} \langle S_{h\nu} S_{\nu\nu}^* \rangle^F - \text{Re} \langle S_{\nu h} S_{\nu\nu}^* \rangle^F \right) \\ &\quad \times \sin^3 \Omega \cos \Omega \\ &\quad + \frac{1}{4} \left( \langle S_{h\nu} S_{h\nu}^* \rangle^F - 2 \text{Re} \langle S_{h\nu} S_{\nu h}^* \rangle^F \right. \\ &\quad \left. + \langle S_{\nu h} S_{\nu h}^* \rangle^F \right) \sin^2 2\Omega \end{aligned} \quad (11a)$$

$$\begin{aligned}
 \langle S_{\nu\nu} S_{\nu\nu}^* \rangle &= \langle S_{\nu\nu} S_{\nu\nu}^* \rangle^F \cos^4 \Omega + \langle S_{hh} S_{hh}^* \rangle^F \\
 &\quad \times \sin^4 \Omega - 2 \operatorname{Re} \langle S_{hh} S_{\nu\nu}^* \rangle^F \sin^2 \Omega \cos^2 \Omega \\
 &\quad + 2 \left( \operatorname{Re} \langle S_{h\nu} S_{\nu\nu}^* \rangle^F - \operatorname{Re} \langle S_{\nu h} S_{\nu\nu}^* \rangle^F \right) \\
 &\quad \times \sin \Omega \cos^3 \Omega \\
 &\quad - 2 \left( \operatorname{Re} \langle S_{hh} S_{h\nu}^* \rangle^F - \operatorname{Re} \langle S_{hh} S_{\nu h}^* \rangle^F \right) \\
 &\quad \times \sin^3 \Omega \cos \Omega \\
 &\quad + \frac{1}{4} \left( \langle S_{h\nu} S_{h\nu}^* \rangle^F - 2 \operatorname{Re} \langle S_{h\nu} S_{\nu h}^* \rangle^F \right. \\
 &\quad \quad \left. + \langle S_{\nu h} S_{\nu h}^* \rangle^F \right) \sin^2 2\Omega \quad (11b)
 \end{aligned}$$

$$\begin{aligned}
 \langle S_{h\nu} S_{h\nu}^* \rangle &= \langle S_{h\nu} S_{\nu h}^* \rangle = \langle S_{\nu h} S_{\nu h}^* \rangle \\
 &= \frac{1}{4} \left( \langle S_{h\nu} S_{h\nu}^* \rangle^F + 2 \operatorname{Re} \langle S_{h\nu} S_{\nu h}^* \rangle^F \right. \\
 &\quad \left. + \langle S_{\nu h} S_{\nu h}^* \rangle^F \right) \quad (11c)
 \end{aligned}$$

$$\begin{aligned}
 \operatorname{Re} \langle S_{hh} S_{\nu\nu}^* \rangle &= \operatorname{Re} \langle S_{hh} S_{\nu\nu}^* \rangle^F (\sin^4 \Omega + \cos^4 \Omega) \\
 &\quad - \frac{1}{4} \left( \langle S_{hh} S_{hh}^* \rangle^F + \langle S_{\nu\nu} S_{\nu\nu}^* \rangle^F \right) \sin^2 2\Omega \\
 &\quad + \frac{1}{4} \left( \operatorname{Re} \langle S_{hh} S_{h\nu}^* \rangle^F + \operatorname{Re} \langle S_{h\nu} S_{\nu\nu}^* \rangle^F \right. \\
 &\quad \quad \left. - \operatorname{Re} \langle S_{hh} S_{\nu h}^* \rangle^F - \operatorname{Re} \langle S_{\nu h} S_{\nu\nu}^* \rangle^F \right) \\
 &\quad \times \sin 4\Omega + \frac{1}{4} \left( \langle S_{h\nu} S_{h\nu}^* \rangle^F - 2 \operatorname{Re} \langle S_{h\nu} S_{\nu h}^* \rangle^F \right. \\
 &\quad \quad \left. + \langle S_{\nu h} S_{\nu h}^* \rangle^F \right) \sin^2 2\Omega \quad (11d)
 \end{aligned}$$

$$\begin{aligned}
 \operatorname{Im} \langle S_{hh} S_{\nu\nu}^* \rangle &= \operatorname{Im} \langle S_{hh} S_{\nu\nu}^* \rangle^F \cos 2\Omega \\
 &\quad + \frac{1}{2} \left( \operatorname{Im} \langle S_{hh} S_{h\nu}^* \rangle^F + \operatorname{Im} \langle S_{h\nu} S_{\nu\nu}^* \rangle^F \right. \\
 &\quad \quad \left. - \operatorname{Im} \langle S_{hh} S_{\nu h}^* \rangle^F - \operatorname{Im} \langle S_{\nu h} S_{\nu\nu}^* \rangle^F \right) \\
 &\quad \times \sin 2\Omega \quad (11e)
 \end{aligned}$$

$$\begin{aligned}
 \operatorname{Re} \langle S_{hh} S_{h\nu}^* \rangle &= \operatorname{Re} \langle S_{hh} S_{\nu h}^* \rangle \\
 &= \frac{1}{2} \left( \operatorname{Re} \langle S_{hh} S_{h\nu}^* \rangle^F + \operatorname{Re} \langle S_{hh} S_{\nu h}^* \rangle^F \right) \cos^2 \Omega \\
 &\quad - \frac{1}{2} \left( \operatorname{Re} \langle S_{h\nu} S_{\nu\nu}^* \rangle^F + \operatorname{Re} \langle S_{\nu h} S_{\nu\nu}^* \rangle^F \right) \sin^2 \Omega \\
 &\quad + \frac{1}{4} \left( \langle S_{h\nu} S_{h\nu}^* \rangle^F - \langle S_{\nu h} S_{\nu h}^* \rangle^F \right) \sin 2\Omega \quad (11f)
 \end{aligned}$$

$$\begin{aligned}
 \operatorname{Im} \langle S_{hh} S_{h\nu}^* \rangle &= \operatorname{Im} \langle S_{hh} S_{\nu h}^* \rangle \\
 &= \frac{1}{2} \left( \operatorname{Im} \langle S_{hh} S_{h\nu}^* \rangle^F + \operatorname{Im} \langle S_{hh} S_{\nu h}^* \rangle^F \right) \cos^2 \Omega \\
 &\quad + \frac{1}{2} \left( \operatorname{Im} \langle S_{h\nu} S_{\nu\nu}^* \rangle^F + \operatorname{Im} \langle S_{\nu h} S_{\nu\nu}^* \rangle^F \right) \sin^2 \Omega \\
 &\quad + \frac{1}{2} \operatorname{Im} \langle S_{h\nu} S_{\nu h}^* \rangle^F \sin 2\Omega \quad (11g)
 \end{aligned}$$

$$\begin{aligned}
 \operatorname{Re} \langle S_{h\nu} S_{\nu\nu}^* \rangle &= \operatorname{Re} \langle S_{\nu h} S_{\nu\nu}^* \rangle \\
 &= \frac{1}{2} \left( \operatorname{Re} \langle S_{h\nu} S_{\nu\nu}^* \rangle^F + \operatorname{Re} \langle S_{\nu h} S_{\nu\nu}^* \rangle^F \right) \cos^2 \Omega \\
 &\quad - \frac{1}{2} \left( \operatorname{Re} \langle S_{hh} S_{h\nu}^* \rangle^F + \operatorname{Re} \langle S_{hh} S_{\nu h}^* \rangle^F \right) \sin^2 \Omega \\
 &\quad + \frac{1}{4} \left( \langle S_{h\nu} S_{h\nu}^* \rangle^F - \langle S_{\nu h} S_{\nu h}^* \rangle^F \right) \sin 2\Omega \quad (11h)
 \end{aligned}$$

$$\begin{aligned}
 \operatorname{Im} \langle S_{h\nu} S_{\nu\nu}^* \rangle &= \operatorname{Im} \langle S_{\nu h} S_{\nu\nu}^* \rangle \\
 &= \frac{1}{2} \left( \operatorname{Im} \langle S_{h\nu} S_{\nu\nu}^* \rangle^F + \operatorname{Im} \langle S_{\nu h} S_{\nu\nu}^* \rangle^F \right) \cos^2 \Omega \\
 &\quad + \frac{1}{2} \left( \operatorname{Im} \langle S_{hh} S_{h\nu}^* \rangle^F + \operatorname{Im} \langle S_{hh} S_{\nu h}^* \rangle^F \right) \sin^2 \Omega \\
 &\quad - \frac{1}{2} \operatorname{Im} \langle S_{h\nu} S_{\nu h}^* \rangle^F \sin 2\Omega. \quad (11i)
 \end{aligned}$$

As shown in (6), Freeman [9] pointed out that because the values of  $\tan^{-1}$  lie between  $\pm\pi/2$ , the FR's  $\Omega$  estimated by (6) should be between  $\pm\pi/4$ . It means that the  $\Omega$  can only be estimated modulo  $\pi/2$ , which is not sufficient. It leaves a  $\pm\pi/2$  ambiguity error in  $\Omega$  because the periodicity of FR effect is  $180^\circ$ .

The  $\pm\pi/2$  ambiguity error makes undetermined inversion as (assuming that the true FR degree is  $\Omega + n\pi/2$ )

$$\begin{aligned}
 \tilde{S}_{\nu\nu} &= S_{\nu\nu} \text{ (when } n \text{ is even) or } -S_{hh} \text{ (when } n \text{ is odd)} \\
 \tilde{S}_{hh} &= S_{hh} \text{ (when } n \text{ is even) or } -S_{\nu\nu} \text{ (when } n \text{ is odd)} \\
 \tilde{S}_{h\nu} &= S_{h\nu}. \quad (12)
 \end{aligned}$$

Similarly, there exists  $\pm\pi/2$  ambiguity error of  $\Omega$  in (10). Thus, the coherency matrix  $\bar{\bar{T}}^\pm$  indicated by undetermined sign  $\pm$  [corresponding to even or odd  $n$  in (12)] is written as

$$\bar{\bar{T}}^\pm = \begin{bmatrix} T_{11} & \pm T_{12} & \pm T_{13} \\ \pm T_{21} & T_{22} & T_{23} \\ \pm T_{31} & T_{32} & T_{33} \end{bmatrix} \quad (13)$$

where  $T_{ij}$  denotes the element of coherency matrix without FR and ambiguity. Correspondingly, the eigenvectors of  $\bar{\bar{T}}^\pm$  are written as

$$\bar{k}_{Pi}^\pm = \begin{bmatrix} \pm k_{Pi,1} \\ k_{Pi,2} \\ k_{Pi,3} \end{bmatrix}. \quad (14)$$

It is easy to find that the eigenvalues  $\lambda_i$  of  $\bar{\bar{T}}^\pm$  ( $i = 1, 2, 3$ ) are the same as that of  $\bar{\bar{T}}$ . Thus, the entropy  $H = -\sum_{i=1}^3 P_i \log_3 P_i$  (where  $P_i = (\lambda_i)/(\sum_{i=1}^3 \lambda_i)$ ) and anisotropy  $A = (\lambda_2 - \lambda_3)/(\lambda_2 + \lambda_3)$  derived from the eigenvalues are not affected by the  $\pm\pi/2$  ambiguity error.

Taking the principle eigenvector  $\bar{k}_{P1}^\pm$ , the classification parameter [10],  $\alpha$ , is calculated as

$$\alpha^\pm = \arctan \left( \frac{\sqrt{|k_{P1,2}|^2 + |k_{P1,3}|^2}}{|\pm k_{P1,1}|} \right) = \alpha. \quad (15)$$

Thus, the set of classification parameters  $(\alpha, H, A)$  [10] is also not affected by the  $\pm\pi/2$  ambiguity error.

Making deorientation of the eigenvector  $\bar{k}_{P1}^\pm$ , one obtains

$$\bar{k}_{P1}^{\pm'} = \begin{bmatrix} \pm k_{P1,1} \\ k_{P1,2} \cos 2\varphi_m + k_{P1,3} \sin 2\varphi_m \\ -k_{P1,2} \sin 2\varphi_m + k_{P1,3} \cos 2\varphi_m \end{bmatrix} \quad (16)$$

where  $\varphi_m$  is the deorientation angle of the polarization base to minimize the cross-polarized scattering [11]. We obtain each element of the scattering matrix from (16)

$$\begin{aligned} S_{hh}^{\pm} &= \frac{\sqrt{2}}{2}(\pm k_{P1,1} + k_{P1,2} \cos 2\varphi_m \\ &\quad + k_{P1,3} \sin 2\varphi_m) = S_{hh} \quad \text{or} \quad -S_{\nu\nu} \\ S_{\nu\nu}^{\pm} &= \frac{\sqrt{2}}{2}(\pm k_{P1,1} - k_{P1,2} \cos 2\varphi_m \\ &\quad - k_{P1,3} \sin 2\varphi_m) = S_{\nu\nu} \quad \text{or} \quad -S_{hh}. \end{aligned} \quad (17)$$

It yields

$$a^{\pm} = \tan^{-1} \left( \frac{|S_{\nu\nu}^{\pm}|}{|S_{hh}^{\pm}|} \right) = a \quad \text{or} \quad \frac{\pi}{2} - a \quad (18)$$

$$b^{\pm} = \frac{1}{2} \arg \left( \frac{S_{\nu\nu}^{\pm}}{S_{hh}^{\pm}} \right) = \pm b. \quad (19)$$

The classification parameters  $u, \nu$  [11] are found as

$$u^{\pm} = \sin c \cos 2a^{\pm} = \pm u \quad (20)$$

$$\nu^{\pm} = \sin c \sin 2a^{\pm} \cos 2b = \nu \quad (21)$$

$$\begin{aligned} \psi^{\pm} &= \begin{cases} \varphi_m, & u^{\pm} > 0 \\ \varphi_m + \frac{\pi}{2}, & u^{\pm} < 0 \end{cases} \\ &= \begin{cases} \varphi_m, \varphi_m + \frac{\pi}{2}, & u < 0 \\ \varphi_m + \frac{\pi}{2}, \varphi_m, & u > 0. \end{cases} \end{aligned} \quad (22)$$

In deorientation classification, the parameters set uses ( $|u|$ ,  $\nu$ ,  $H$ ). Thus, the  $\pm\pi/2$  ambiguity error and the undetermined sign  $\pm$  of  $\bar{T}^{\pm}$  do not affect the classification by the parameters set ( $u, \nu, H$ ) or ( $\alpha, H, A$ ). But the orientation angle  $\psi^{\pm}$  of [11] is affected by  $\pm\pi/2$  ambiguity error.

#### IV. METHOD TO ELIMINATE $\pm\pi/2$ AMBIGUITY ERROR

Freeman [9] proposed four approaches to eliminate  $\pm\pi/2$  ambiguity error.

- 1) To deploy a calibration target (e.g., a transponder) within the scene with polarization signature  $\begin{pmatrix} 1 & 0 \\ 0 & 0 \end{pmatrix}$  or  $\begin{pmatrix} 0 & 0 \\ 0 & 1 \end{pmatrix}$ .
- 2) To examine the polarization signature of a slightly rough surface, for which the  $\nu\nu$  backscattering is typically greater than or equal to the  $hh$ . It might be easily implemented for land surface, simply by initiating or concluding each data-take over the ocean and using that as a benchmark. On the shuttle radar topography mission, all data-takes started and finished over the ocean to provide a calibration reference for surface topography.
- 3) To constrain  $\Omega$  itself by observing when the ionosphere is relatively quiet, e.g., at night during solar minimum for example, and  $\Omega$  may be less than  $45^\circ$  at both L- and P-bands.

- 4) To correlate the dataset with an earlier one, obtained by the same radar under identical viewing conditions, but without FR rotation.

From calculation of (2), Fig. 7(a) shows a global distribution of the FR degree at 6 A.M. on June 1, 1989 based on total electron content and geomagnetic field at that time. Generally, it can be seen that due to the orientation of geomagnetic field, the FR degree is negative on the northern hemisphere, and is positive on the southern hemisphere. It also can be seen that both the geomagnetic field and total electron content gradually change with geographical location, it makes correspondingly smooth change of the FR degree.

The  $\pm\pi/2$  ambiguity comes from the calculation of  $\Omega' = 0.5 \tan^{-1}[\tan 2\Omega]$ . We recalculate  $0.5 \tan^{-1}[\tan 2\Omega]$  for each pixel of Fig. 7(a), and obtain a global distribution of FR degree with  $\pm\pi/2$  ambiguity error as shown in Fig. 7(b). It can be found that Fig. 7(b) is totally deviated from Fig. 7(a).

The solid and dashed lines in Fig. 8 are the true FR and the FR with  $\pm\pi/2$  ambiguity error along the longitude  $150^\circ$  E of Fig. 7(a) and (b), respectively.

The problem of  $\pm\pi/2$  ambiguity is similar to the phase wrapping in interferometric SAR measurement. As an alternative approach to correct the  $\pm\pi/2$  ambiguity error, 1-D phase unwrapping method (integral of phase difference) can be employed to recover the true FR degree.

To recover the true FR degree, a benchmark is defined as the zero FR as shown by a white line in Fig. 7(a), where the angle between the directions of wave propagation and geomagnetic field reaches  $90^\circ$  by (5) and zero FR by (2). Then, a method similar to phase unwrapping is employed to recover the true FR degree on each pixel starting from the points with zero FR.

Similar to unambiguous phase difference condition [14], it is assumed that the difference of the FR degree from its adjacent pixels should be  $|\Delta\Omega| < \pi/4$ . The true FR degree along the longitude (column) is recovered by the following process:

$$\Omega_n = \sum_{i=s}^n (\Delta\Omega_i + k_i\pi/2) + \Omega_s \quad (23a)$$

$$k_i = \begin{cases} 0, & (|\Delta\Omega| \leq \pi/4) \\ -1, & (\Delta\Omega > \pi/4) \\ 1, & (\Delta\Omega < -\pi/4) \end{cases} \quad (23b)$$

where  $\Omega_s$  is the FR degree on the benchmark,  $\Delta\Omega_i$  is the difference of FR degree from adjacent pixels (when  $n > s$ ,  $\Delta\Omega_i = \Omega_i - \Omega_{i-1}$ ; when  $n < s$ ,  $\Delta\Omega_i = \Omega_i - \Omega_{i+1}$ ; when  $n = s$ ,  $\Delta\Omega_i = 0$ ).

Since each column contains a benchmark, the true FR degree of each pixel can be sequentially recovered. Recovered FR degrees from the dashed FR in Fig. 8 are exactly returned to the solid line. Also, global distribution of FR degree without  $\pm\pi/2$  ambiguity error [identical with Fig. 7(a)] can be recovered from Fig. 7(b).

Similarly, some phase unwrapping methods (such as the integral track or least square methods) can be employed to eliminate noise or other disturbances of SAR measurements, which may break FR values.

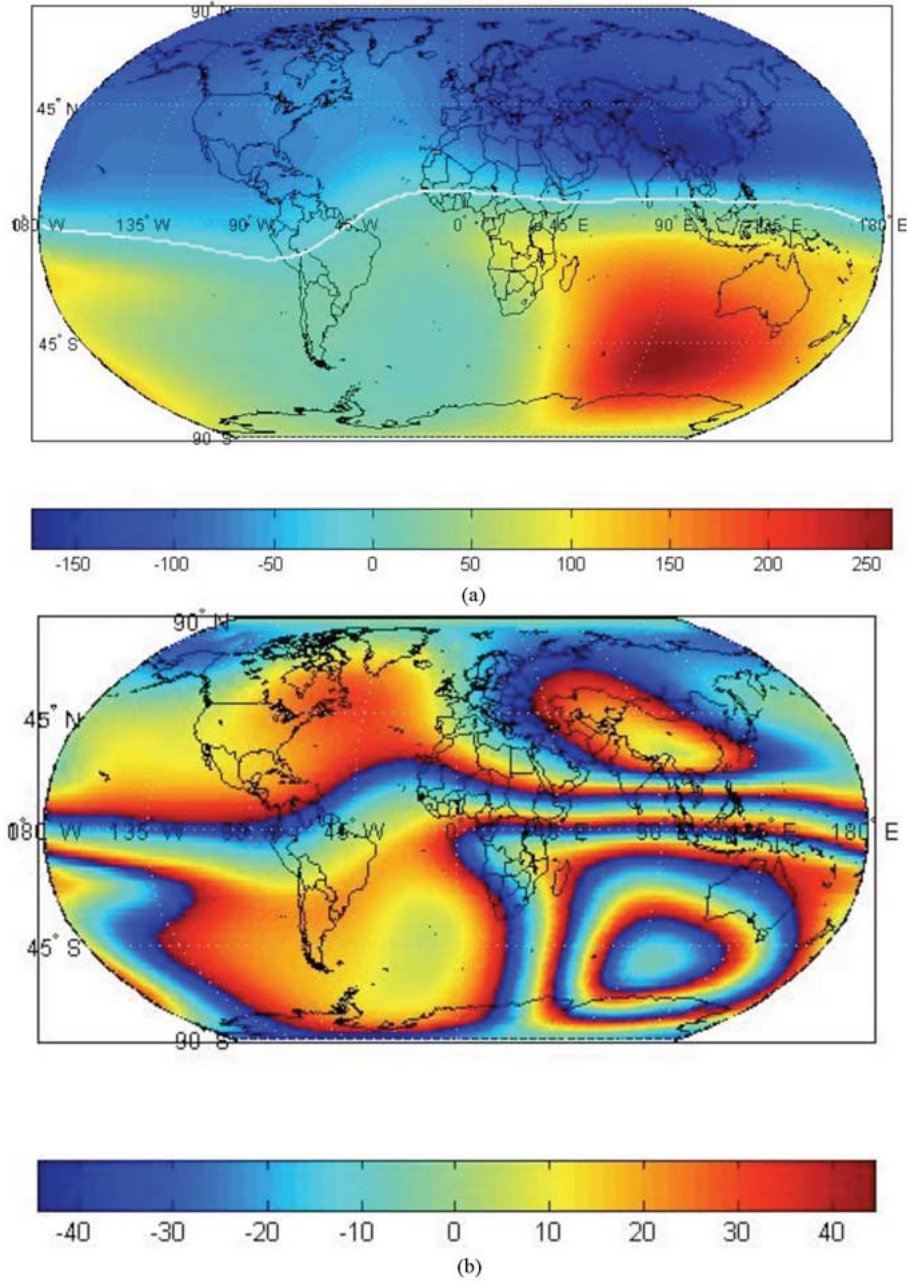


Fig. 7. (a) Global distribution of FR degree at P-band. (b) Global distribution of FR degree at P-band with  $\pm\pi/2$  ambiguity error.

This method involving finding a benchmark area close to the equator might become restrictive because polarimetric SAR data rates tend to be much higher than for conventional single-polarization SARs, and operation in full polarimetric SAR mode is often restricted to a few minutes per orbit. In practice, this would limit the full correction capability to tropical areas only.

However, if there is no zero-FR available, any single point in the image can be chosen as the benchmark. The FR degree of other pixels can be inverted by 2-D phase unwrapping method. These results might not be true, but are only different from the true values with the integer multiples of  $\pi/2$  as the same as the benchmark. These inverted polarimetric data might be correct, or all keep the same  $\pm\pi/2$  ambiguity error. Further, based

on criterion  $\langle |S_{\nu\nu}|^2 \rangle > \langle |S_{hh}|^2 \rangle$  in some known areas such as ocean, the  $\pm\pi/2$  ambiguity in those points can be resolved, as suggested by [9]. Those points can be also chosen as the benchmark for the phase unwrapping.

## V. CONCLUSION

- 1) Polarimetric SAR measurement with FR at low frequency such as P-band cannot be directly applied to surface classification.
- 2) The scattering and Mueller matrices can be derived with the  $\pm\pi/2$  ambiguity error from those with FR, and applicable to surface classifications by using the parameters  $u, \nu, H, \alpha, A$ .



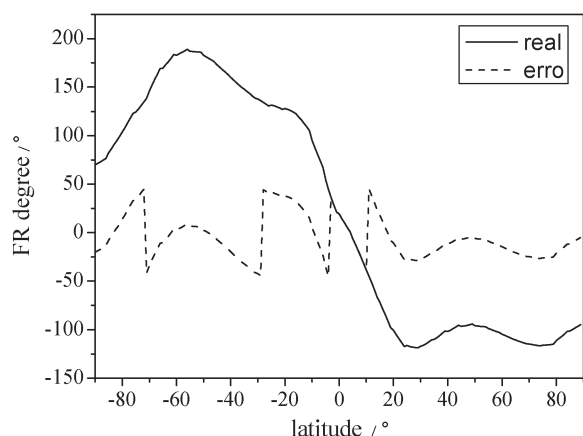


Fig. 8. FR degree along the longitudes 150° E.

- 3) Based on gradual change of FR degree and zero FR as a starting point, similar to the phase unwrapping method, then the  $\pm\pi/2$  ambiguity error can be eliminated. Thus, the true FR degree and polarimetric data without any FR effect can be recovered.
- 4) Two-dimensional phase unwrapping method with the benchmark at some well-known areas can be employed to resolve the  $\pm\pi/2$  ambiguity error when no zero FR is contained in SAR image data.
- 5) All discussion and approach can be applied to even lower VHF bands.

## REFERENCES

- [1] M. C. Dobson *et al.*, "Dependence of radar backscatter on conifer forest biomass," *IEEE Trans. Geosci. Remote Sens.*, vol. 30, no. 2, pp. 412–415, Mar. 1992.
- [2] E. Rignot, R. Zimmermann, J. van Zyl, and R. Oren, "Spaceborne applications of a P-band imaging Radar for mapping of forest biomass," *IEEE Trans. Geosci. Remote Sens.*, vol. 33, no. 5, pp. 1162–1169, Sep. 1995.
- [3] M. Moghaddam, S. Saatchi, and R. H. Cuenca, "Estimating subcanopy soil moisture with radar," *J. Geophys. Res.*, vol. 105, no. D11, pp. 14 899–14 911, Jun. 2000.
- [4] A. Freeman, S. L. Durden, and R. Zimmermann, "Mapping subtropical vegetation using multifrequency, multipolarization SAR data," in *Proc. IGARSS*, Houston, TX, 1992, pp. 1986–1989.
- [5] M. Moghaddam, E. Rodriguez, Y. Rahmat-Samii, D. Moller, J. Hoffman, J. Huang, and S. Saatchi, "Microwave observatory of subcanopy and subsurface (MOSS): A low-frequency radar for global deep soil moisture measurements," in *Proc. IGARSS*, Jul. 2003, vol. 1, pp. 500–502.
- [6] L. Pierce and M. Moghaddam, "A tower-based prototype UHF/VHF radar for subcanopy and subsurface soil moisture," in *Proc. IGARSS*, Seoul, Korea, Jun. 25–28, 2005.
- [7] D. M. Le Vine and S. Abraham, "The effect of the ionosphere on remote sensing of sea surface salinity from space: Absorption and emission at L Band," *IEEE Trans. Geosci. Remote Sens.*, vol. 40, no. 4, pp. 771–782, Apr. 2002.
- [8] P. A. Wright *et al.*, "Faraday rotation effects on L-Band spaceborne SAR data," *IEEE Trans. Geosci. Remote Sens.*, vol. 41, no. 12, pp. 2735–2744, Dec. 2003.
- [9] A. Freeman, "Calibration of linearly polarized polarimetric SAR data subject to Faraday rotation," *IEEE Trans. Geosci. Remote Sens.*, vol. 42, no. 8, pp. 1617–1624, Aug. 2004.
- [10] E. Pottier and J. S. Lee, "Application of the H/A/alpha polarimetric decomposition theorem for unsupervised classification of fully polarimetric SAR data based on the Wishart distribution," in *Proc. Committee Earth Observing Satellites SAR Workshop*, Toulouse, France, Oct. 26–29, 1999.
- [11] F. Xu and Y.-Q. Jin, "Deorientation theory of polarimetric scattering targets and application to terrain surface classification," *IEEE Trans. Geosci. Remote Sens.*, vol. 43, no. 10, pp. 2351–2364, Oct. 2005.
- [12] J. A. Kong, *Electromagnetic Wave Theory*. New York: Wiley-Interscience, 1985.
- [13] A. Freeman and S. S. Saatchion, "The detection of Faraday rotation in linearly polarized L-Band SAR backscatter signatures," *IEEE Trans. Geosci. Remote Sens.*, vol. 40, no. 8, pp. 1607–1616, Aug. 2004.
- [14] G. Fornaro *et al.*, "Phase difference based multiple acquisition phase unwrapping," in *Proc. IGARSS*, Toulouse, France, 2003, vol. 2, pp. 948–950.
- [15] L. Li and F. Li, "Effect of Faraday rotation on polarimetric SAR backscattering signatures based on four-component scattering model," *IEEE Geosci. Remote Sens. Lett.*, 2006, submitted for publication.



**Ren-Yuan Qi** received the B.S. degree from East China Normal University, Shanghai, in 2005. He is currently working toward the M.S. degree at Fudan University, Shanghai.

His main research interests include radar polarimetry, electromagnetic scattering modeling, and information retrieval on remote sensing.

Mr. Qi received the prize of National Undergraduate Electronic Design Contest in 2003.



**Ya-Qiu Jin** (SM'89–F'04) received the B.S. degree from Peking University, Beijing, China, in 1970, and the M.S., E.E., and Ph.D. degrees from the Massachusetts Institute of Technology, Cambridge, in 1982, 1983, and 1985, respectively.

He was a Research Scientist with the Atmospheric and Environmental Research, Inc., Cambridge, MA (1985); a Research Associate with the City University of New York (1986–1987); a Visiting Professor with the University of York, U.K. (1993–1994), sponsored by the U.K. Royal Society; a Visiting Professor with the City University of Hong Kong (2001); and a Visiting Professor with Tohoku University, Japan (2005). He held the Senior Research Associateship at National Oceanic and Atmospheric Administration (NOAA)/National Environmental Satellite, Data, and Information Service (NESDIS) awarded by the National Research Council (1996). He is currently a Professor with the School of Information Science and Engineering, and the Director of the Key Laboratory of Wave Scattering and Remote Sensing Information (Ministry of Education), Fudan University, Shanghai, China. He has been appointed as the Principal Scientist for the China State Key Basic Research Project (2001–2006) by the Ministry of National Science and Technology of China to lead the remote-sensing program in China. He has published more than 510 papers in China and abroad, and eight books, three of which are in English: *Electromagnetic Scattering Modeling for Quantitative Remote Sensing* (World Scientific, 1994), *Information of Electromagnetic Scattering and Radiative Transfer in Natural Media* (Science Press, 2000), and *Theory and Approach for Information Retrieval from Electromagnetic Scattering and Remote Sensing* (Springer, 2005). He is the Editor of The International Society for Optical Engineers Volume 3503 *Microwave Remote Sensing of the Atmosphere and Environment*, and the book *Wave Propagation, Scattering and Emission in Complex Media* (World Scientific and Science Press, 2004). His main research interests include scattering and radiative transfer in complex natural media, microwave remote sensing, as well as theoretical modeling, information retrieval and applications in atmosphere, ocean, and Earth surfaces, and computational electromagnetics.

Dr. Jin was elected IEEE Fellow for his contributions to electromagnetic scattering model for remote-sensing applications. He is Chairman of IS-APE2000, the Specialist Workshop 2004 on Electromagnetic (EM) Scattering and Information Retrieval in Remote Sensing, and the 6th Asia-Pacific Engineering Research Forum on Microwaves and Electromagnetic Theory Workshop (2006). He is the Founder and Chairman of the IEEE Geoscience and Remote Sensing Society (GRSS) Beijing Chapter (1998–2003) and received the appreciation for his notable service and contributions toward the advancement of IEEE professions from IEEE GRSS. He is an Associate Editor of the IEEE TRANSACTIONS ON GEOSCIENCE AND REMOTE SENSING. He received the China National Science Prize in 1993, the First-Grade Science Prizes of the Ministry of Education in 1992 and 1996, the State Book Prize in 1997, the Teaching Excellence Prize of Shanghai City in 2001, the Excellent Supervisor for Graduate Students in Fudan University in 2003, and the Fudan President Prize in 2004, among other many prizes.